The application of molecular simulation to the rational design of new materials: 1. Structure and modelling studies of linear epoxy systems

J. M. Barton
Materials and Structures Department, Defence Research Agency (Aerospace Division) RAE, Farnborough, Hampshire, GU14 6TD, UK

and G. J. Buist, A. S. Deazle, I. Hamerton, B. J. Howlin* and J. R. Jones
Department of Chemistry, University of Surrey, Guildford, Surrey, GU2 5XH, UK
(Received 28 December 1992; revised 10 February 1994)

The variation in torsional angles for a model linear epoxy system was studied as a function of applied stress and temperature. It was found that all of the torsional angles demonstrate a population migration from a lower to a higher energy state upon the application of an external stress. Subtle changes in torsional angle values under these conditions result in large energy differences.

(Keywords: linear epoxy system; torsional angles; conformational analysis)

INTRODUCTION

Epoxy resins are a very versatile family of polymers that are converted to thermoset products through reaction with well over fifty different classes of chemical compounds[1]. Bisphenol A and epichlorohydrin form the basis of these widely used commercial resins which find application in such diverse areas as protective coatings and structural applications (e.g. laminates and composites, tooling, moulding, casting, construction, bonding and adhesives). As they have low molecular weights these epoxide resins[2] need to be crosslinked to make them into useful products. Linear amines (primary and secondary) are generally used as low-cost and low-viscosity crosslinking agents (hardeners). Aromatic amines, however, have a much lower activity than the aliphatic amines, and are therefore used for high temperature curing (usually at $\sim 150°C$) systems to produce cured resins with good strength and chemical resistance.

The amine-induced cure of epoxides and the subsequent crosslinking chemistry is very complex, and a number of competing reactions have been identified[3–5]. These reactions depend on the ratio of the amount of curing agent to the amount of epoxy-containing moiety. Using stoichiometric amounts, addition reactions take place, which with multifunctional curing agents and epoxy moieties lead to three-dimensional, crosslinked networks. With catalytic amounts, the epoxy moieties undergo homopolymerization, but this reaction can also occur on raising the temperature of the previous systems. As part of our continuing interest in the structure and mechanisms of epoxy resins, we have studied the kinetics of the stoichiometric reaction by using a novel radiochemical method[6], and are currently studying the homopolymerization reaction with novel transition-metal-containing catalyst[7–9]. Our previous work on the stoichiometric reaction[6] was concerned with model chemical compounds that were unable to form the long chains that are characteristic of fully cured epoxy resins, and so the logical extension was to increase the complexity of the systems so as to enable chain formation, but also to prevent crosslinking which makes the system relatively intractable from a chemical analysis point of view. Hence, the curing agent, 1,2-dianilinoethane, was chosen for this study as it has two reactive hydrogens to complex, but lacks the ability to crosslink. The epoxy moiety chosen was the bisphenol A of diglycidyl ether (BADGE), one of the commonest materials used in aerospace applications. The study was performed on two fronts, which concerned both the chemical properties, and a computational simulation of the cured materials. The work presented here demonstrates the changes in conformation of an epoxy link under compressive and tensile stress. Changes in the torsional angles are the most important and main contributors to the conformational changes in this epoxy link. The distribution of these torsional angles is important, and will be calculated and characterized in this paper. The torsional angles of interest are defined in *Figure 1*. Due to the difficulty in determining the validity of the proposed localized minima, from molecular dynamics (MD) and conformational analysis, comparisons will be made with analogous crystal data.

* To whom correspondence should be addressed

0032-3861/94/20/4326–08

EXPERIMENTAL

Crystal data

The crystal data for the torsional angles were obtained by searching the Cambridge Structural Database (Version 3)[10] for structures containing fragments of the link segment that is shown in *Figure 1*. An individual fragment was used to duplicate each torsional angle including any substituents.

Table 1 summarizes the torsional angle values and the search distribution results. The torsional values that were found were rounded to the nearest 10°, as the conformational analysis was conducted at 10° intervals. (A list of reference codes from the Cambridge Database search can be obtained from the authors on request.)

Simulation techniques

Model. The computer program 'POLYGRAF' (produced by Molecular Simulation, Inc.), using a Stardent Tital 2 graphics mini-supercomputer, was employed to model the product of the reaction between the BADGE and 1,2-dianilinoethane (i.e. the unit shown in *Figure 1*). The inherent symmetry of the models is used to duplicate the torsional angles of interest. The generic force field, Drieding-II, which was used in this work has been described previously[11]. The forms of the potential energy functions for bond stretching, angle bending, torsions and inversion, are given, respectively, as:

$$E_b = \tfrac{1}{2}K_b(R - R_0)^2 \quad (1)$$

$$E_a = \tfrac{1}{2}K_a(\theta - \theta_0)^2 \quad (2)$$

$$E_\theta = \tfrac{1}{2}V_{jk}\{1 - \cos[n_{jk}(\phi - \phi_e)]\} \quad (3)$$

$$E_\omega = \tfrac{1}{2}C(\cos\omega - \cos\omega_0)^2 \quad (4)$$

where K_b and K_a are the force constants for bond stretching and angle bending, and R_0 and θ_0 are the equilibrium bond length and bond angle, respectively. In equation (3), E_θ represents the torsional angle interaction potential between the two bonds ij and kl which are connected through a common bond, jk, and the angle between the planes ijk and jkl is the dihedral angle ϕ while V_{jk} is the rotational barrier, n_{jk} is the multiplicity and ϕ_e is the equilibrium value of the dihedral angle. In

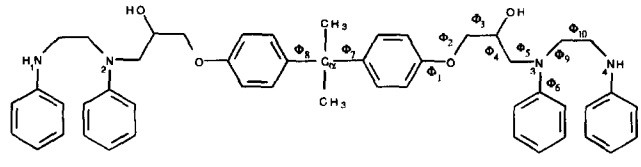

Figure 1 Structure of the linear epoxy link segment

Table 1 Distribution of the 'hits' made during the Cambridge Structural Database search, where the numbers given are percentage values for the total number of hits at a given torsional angle value

Angle (deg)	Φ_1	Φ_2	Φ_3	Φ_4	Φ_5	Φ_6	Φ_7, Φ_8	Φ_9	Φ_{10}
−180	27.3	37.5	15.3	12.5					
−170	9.1	25	13.6	12.5	12.5	7.1			
−160			3.4						
−150							2.9		
−140							5.9		
−130							5.9		
−120							17.6		
−110							2.9		
−100						7.1			
−90						7.1			
−80			1.7		12.5			100	
−70			5.1	6.3	12.5				100
−60			6.8	12.5			8.8		
−50			3.4				5.9		
−40							5.9		
−20						14.3			
−10	18.2				12.5	7.1			
0						14.3			
10	4.5				12.5	35.7			
50			3.4			7.1	14.7		
60			16.9				14.7		
70			1.7		12.5				
110							5.9		
130					12.5		5.9		
140							2.9		
150	4.5								
170	13.6	18.8	16.9	31.3	12.5				
180	22.7	18.8	11.9	25					
No. of hits	22	16	59	16	8	14	34	1	1

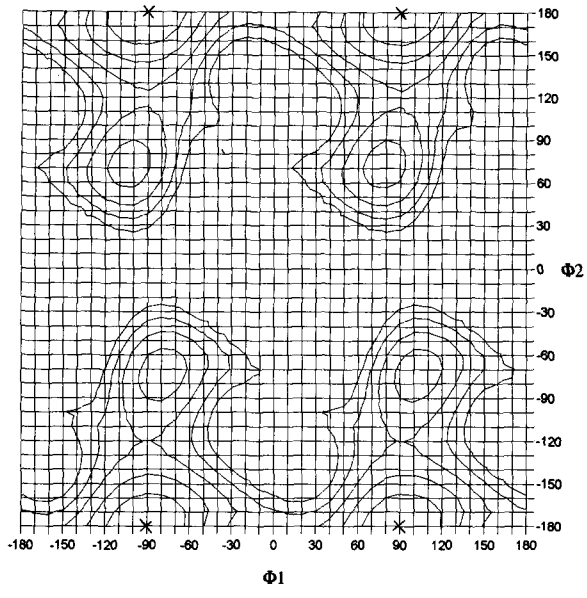

Figure 2 Conformational energy plot for rotations about torsional bonds 1 and 2. The minima are marked by crosses and the contours are at 1 kcal mol^{-1} intervals above the minima

this paper, the *trans*-configuration corresponds to $\Phi = 180°$. Equation (4) is the energy function for the inversion angle, where $k_\omega = C \sin^2 \omega_0$ is the force constant and ω is the angle of an atom which is out of plane. This can be readily depicted by the three atoms j, k, l, connected to a common atom i. When all of the atoms lie flat on a plane, then $\omega = 0$; if the atom j, for example, moves out of the plane, ω is the angle between the plane and the new bond position ij. The van der Waals interaction is represented through a Lennard-Jones 12-6 potential;

$$E_{vdw}(R) = D_0\left[\left(\frac{R_0}{R}\right)^{12} - 2\left(\frac{R_0}{R}\right)^{6}\right] \quad (5)$$

The hydrogen bonding function is the Lennard-Jones 12-10 potential, which is described below:

$$E_{hb}(D_0)\left[5\left(\frac{R_0}{R}\right)^{12} - 6\left(\frac{R_0}{R}\right)^{10}\right] \quad (6)$$

where D_0 is the hydrogen bond strength (well depth) in kcal mol^{-1}, R is the distance (in Å) between the donor and acceptor atom, while R_0 is the equilibrium length (in Å). There is a switching function which smoothly cuts off the interaction, using an on-distance at 8 Å and an off-distance at 8.5 Å. E_{ele}, in equation (7) below, is the electrostatic energy between two bodies with charges Q_i and Q_j, which are separated by a distance R_{ij}, while ε is the dielectric constant and C_0 is a conversion factor, giving E_{elec} in kcal mol^{-1} as follows:

$$E_{elec} = C_0 \sum_{i>j} \frac{Q_i Q_j}{\varepsilon R_{ij}} \quad (7)$$

The torsional angles, Φ_1–Φ_8, from the model depicted in *Figure 1*, were initially set to the following values, namely 0, 180, −60, 180, 90, 0, 52 and 52°, respectively. These are the conformational values for the energy minima collected from the literature[12,13]. Further minimization of our model in this 'minimized' conformation results in changes being seen in Φ_1, Φ_3, Φ_4, Φ_5 and Φ_6. The torsional values of our minimized structure coincided with the low energy regions from our conformational analysis data (this will be discussed later).

One hundred and fifty conformations of the kind depicted in *Figure 1* were generated using the Monte Carlo technique. By the nature of the algorithm, high energy conformers were rejected using a van der Waals (vdw) checking procedure between the atoms. Fifteen of the lowest energy conformations were selected for further experimental work. These conformers were then changed by using the Gasteiger method[14]. A wide range of low energy conformers are required to obtain a good distribution of values for each torsional angle, without biasing any conformational results.

Simulation I. A conformational search between all adjacent torsional angle pairs was calculated. A pair of torsional angles were stepped from 0 to 350°, at 10° intervals. After each step, the pair of torsional angles were held stationary while the remainder of the molecule was minimized to energy convergence (see *Figures 2–6*).

Simulation II. A periodic boundary box was applied to four of the structures whose conformations had previously been generated by the Monte Carlo technique. The following steps were applied during this computer experiment; step 1, the molecule only was energy-minimized, using the conjugate-gradient method, until energy convergence was achieved; step 2, the molecule was allowed to equilibrate at 300 K, at a fixed volume, until the potential energy reached equilibrium, using the summed verlet algorithm[15]; step 3, at this point the conformation with the lowest potential energy was extracted; step 4, the structure was subject to an uniaxial force which was applied to the box face perpendicular to the axis of the link molecule. Separate compressive and tensile stress experiments were then applied to each system. The time step for the molecular dynamics was 1 fs, and 'snapshots' were taken every 0.1 ps during steps 2 and 4. The values of each torsional angle (shown in *Figure 1*) were analysed from the snapshots and are shown as population plots in *Figures 7–11*.

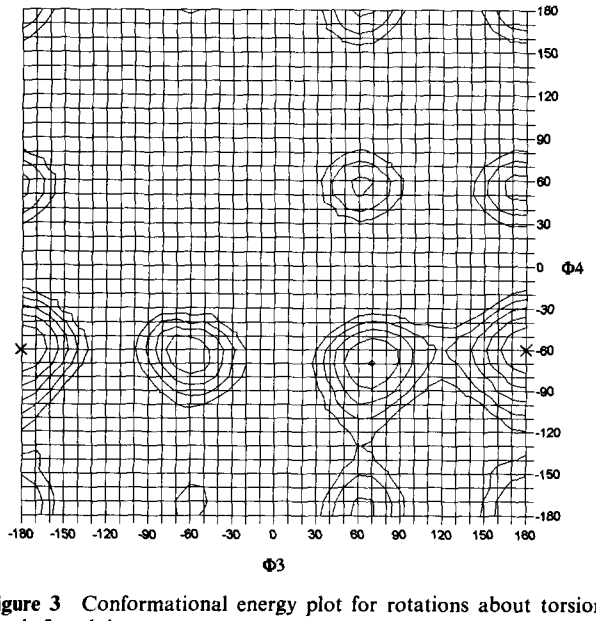

Figure 3 Conformational energy plot for rotations about torsional bonds 3 and 4

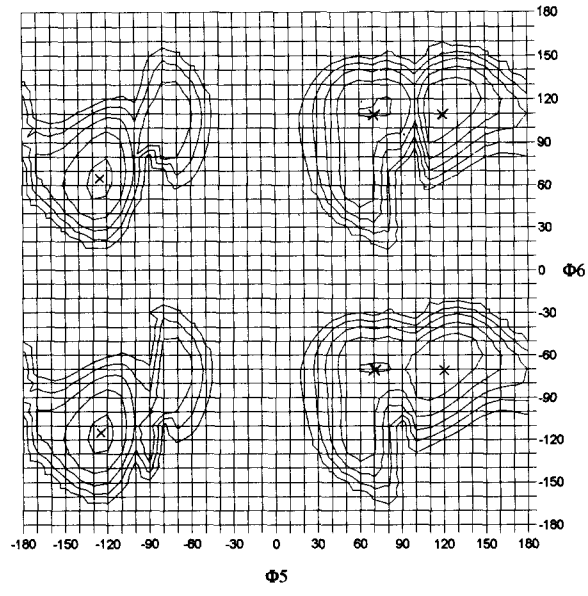

Figure 4 Conformational energy plot for rotations about torsional bonds 5 and 6

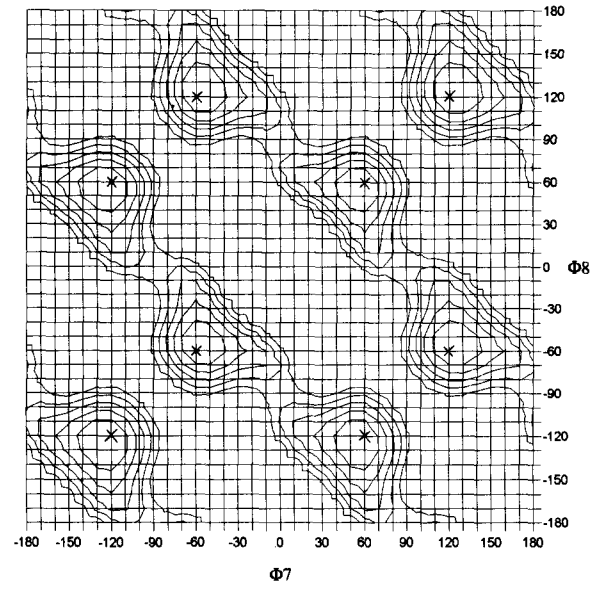

Figure 5 Conformational energy plot for rotations about torsional bonds 7 and 8

RESULTS AND DISCUSSION

The torsional angle Φ_1 deviates significantly from the crystal data. *Ab initio* calculations[16] indicate that the conformation of the O–C bond is approximately co-planar with the phenyl ring. This conformation maximizes the conjugation between the π lone pair on the ether oxygen and the π electrons of the phenyl ring. When $\Phi_1 = 0°$ (or 180°), there is a 9 kcal mol^{-1} increase in the van der Waals energy component. This is due to the close proximity (1.89 Å) of the methylene hydrogens and the phenyl hydrogen. If, however, $\Phi_1 = \pm 90°$, then the total potential energy decreased by ~ 5 kcal mol^{-1}.

There is close agreement between the conformational analysis and molecular dynamics results for Φ_1 at 300 K, indicating a bi-modal system. The torsional values occupied by Φ_1 can be assigned to the $\pm 70°$ region at 300 K (*Figure 7a*). On the application of a compressive stress, the Φ_1 shifts to two degenerate states, which are energetically higher. These two degenerate states can be seen in *Figure 2*. This tetra-modal system resides at the torsional values of $\pm 110°$ and $\pm 60°$ (*Figure 7a*). The energy difference between the ground state at $\pm 70°$ and these higher energy levels is ~ 1–3 kcal mol^{-1}. When the system is expanded, there is a slight shift to $\pm 100°$, but it remains bi-modal, as can be seen in *Figure 7a*.

The majority of the Φ_2 values obtained from the Cambridge Database (CDB) search are at $\pm 180°$, which compares favourably with the minima regions seen in the conformational energy plot (*Figure 2*). From the molecular dynamics runs, the Φ_2 is a tri–modal system with a degenerate state at the torsional values of $\pm 70°$, while the energy minima reside at $\pm 180°$. From the results of the conformational analysis, the degenerate state has a higher energy level, which is between 1–2 kcal mol^{-1} (shown in *Figure 2*). When the system is under expansion, the torsional values at $\pm 180°$ predominate the populated region, in comparison to the degenerate state at $\pm 70°$. The population between $\pm 180°$ and $\pm 70°$ is relatively high, indicating an easier transfer between the states, as shown in *Figure 7b*. Under a compressive stress, a shift takes place and the population at $\pm 70°$ dominates. This results in Φ_1 residing at the torsional values of $\pm 110°$ and $\pm 60°$, which was discussed earlier.

Figure 8a shows that Φ_3 is essentially a tri-modal system, with population regions at ± 180, -60 and 70°. The crystal data and the conformational analysis plot, *Figure 3*, are in total agreement with these populated regions. At 300 K (*Figure 8a*), the region at 80° is highly populated, with this being due to a minima region (0–1 kcal mol^{-1}) at this point for the conformational plot $\Phi_2\Phi_3$ (not shown). There is a potential for intramolecular hydrogen bonding from the hydroxyl hydrogen to the ether group at the minima for Φ_3. The energy of the hydrogen bond was calculated to be -0.24 kcal mol^{-1}. Closer inspection of the energy composition shows that, in this configuration, the hydrogen bonding is a less significant factor than the van der Waals energy. Φ_3 populates all of the low energy population states under

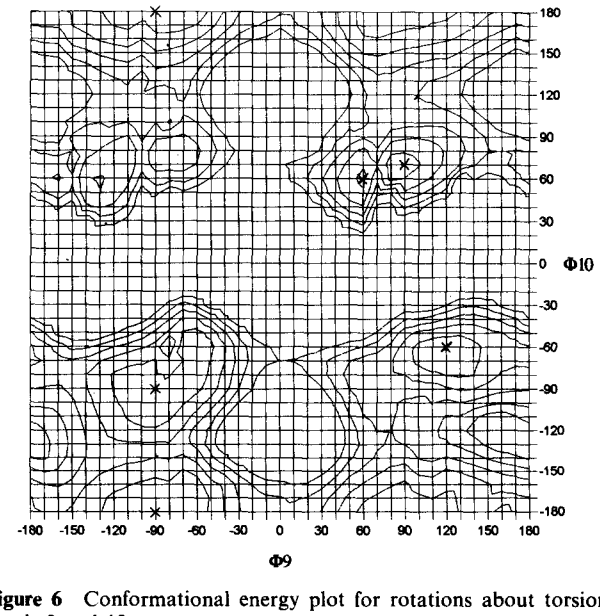

Figure 6 Conformational energy plot for rotations about torsional bonds 9 and 10

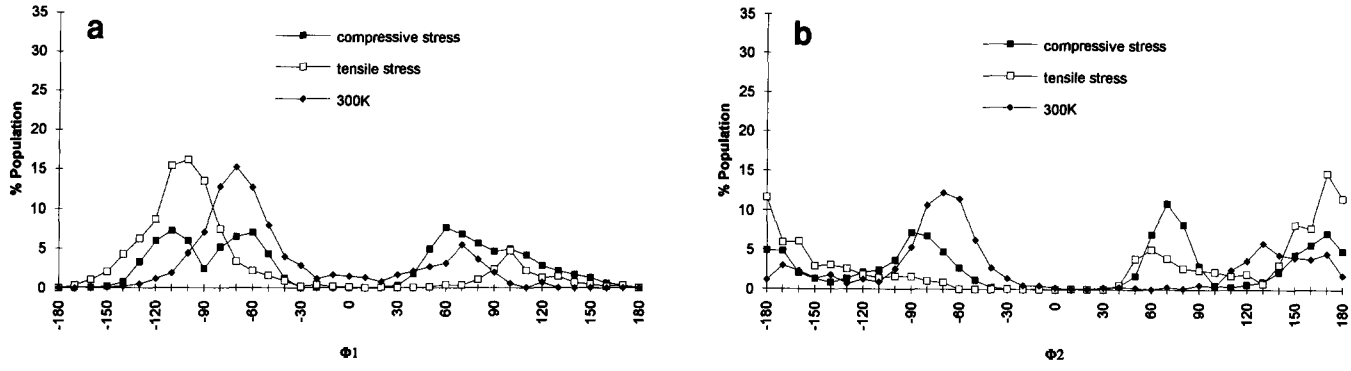

Figure 7 Distribution of (a) torsional bond 1, (b) torsional bond 2, under stress and constant pressure at 300 K

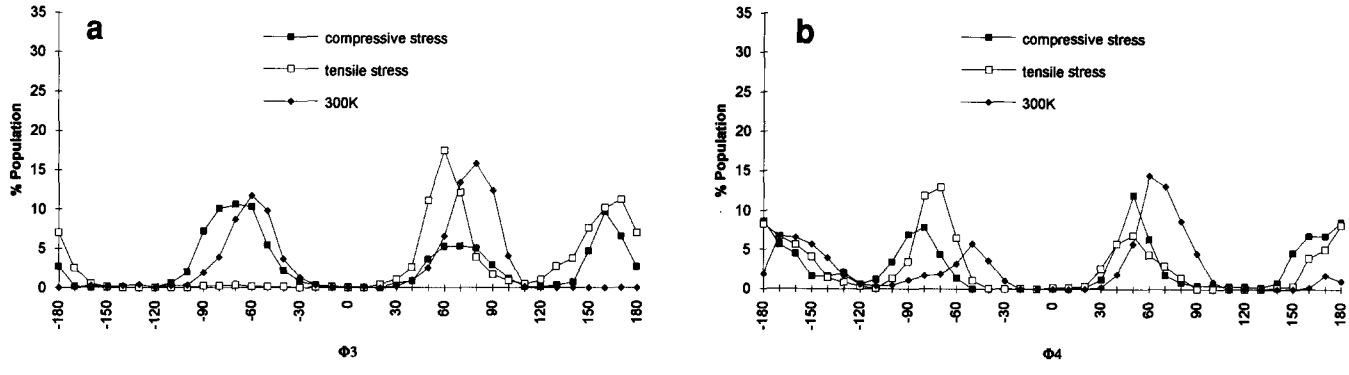

Figure 8 Distribution of (a) torsional bond 3, (b) torsional bond 4 under stress and constant pressure at 300 K

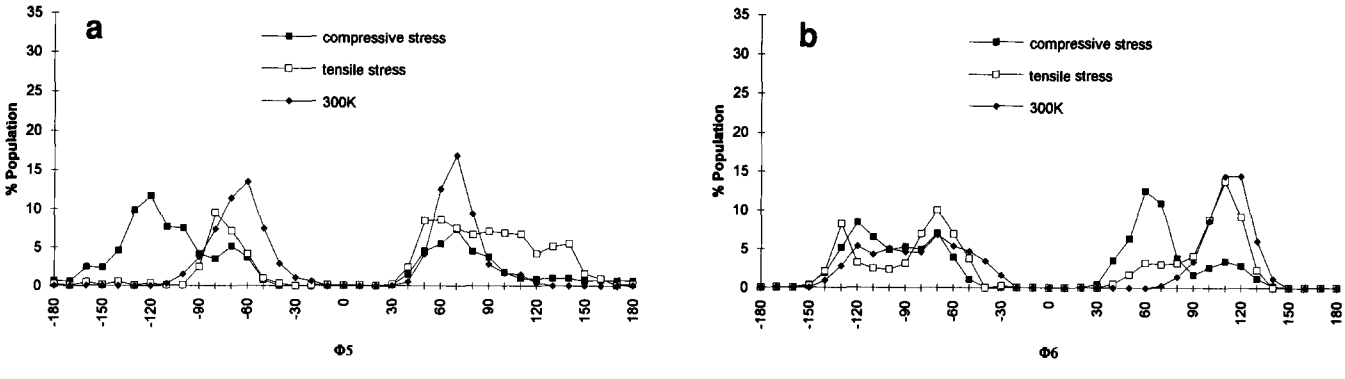

Figure 9 Distribution of (a) torsional bond 5, (b) torsional bond 6, under stress and constant pressure at 300 K

the various conditions. As external stresses are applied, so a shift in the population from one low energy region to another is observed. On the application of a tensile stress, the population at a torsional value of 70° increases at the expense of those at $-70°$ and $\pm 180°$, whereas on compression the $-70°$ region predominates at the expense of the 70° region (see *Figure 8a*).

The torsional angle values which appear in the crystal data for Φ_4, compare favourably with the results from the conformational analysis (*Figure 3*), and molecular dynamics experiments (*Figure 8b*). The $\Phi_3\Phi_4$ conformational analysis plot (*Figure 3*) shows that there is only one region on the plot that is below 1 kcal mol^{-1}. This single mode is situated at the torsional value of $-70°$. Hydrogen bonding, between the hydroxyl and the ether group, is observed at this minimum. The population of

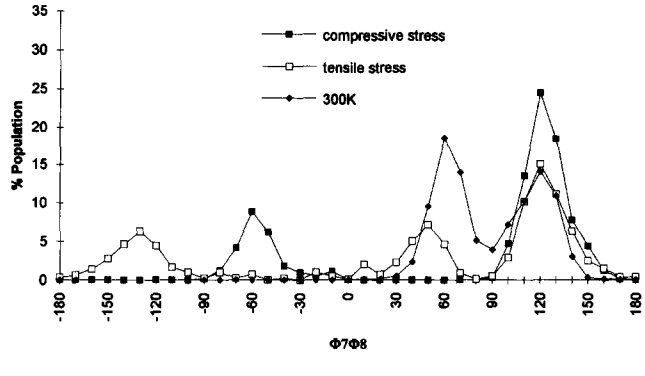

Figure 10 Distribution of torsional bonds 7 and 8, under stress and constant pressure at 300 K

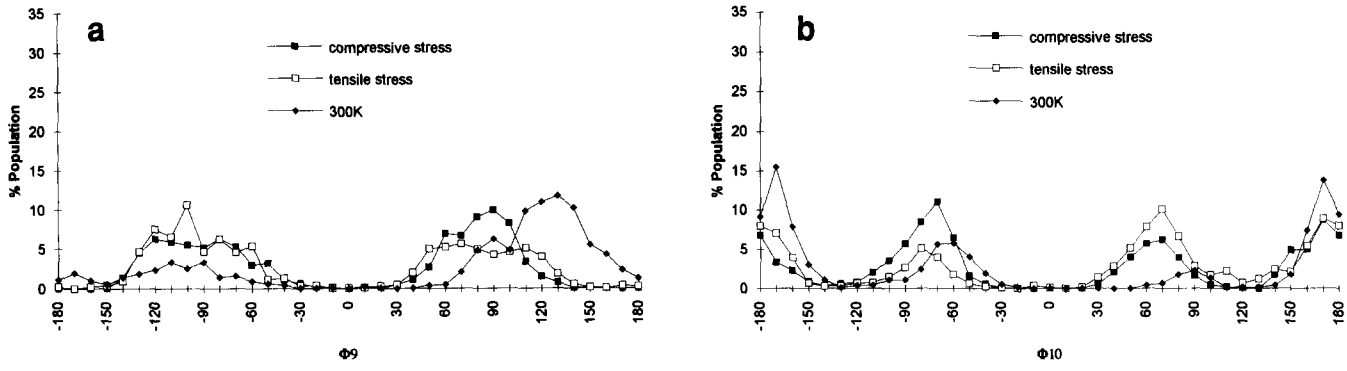

Figure 11 Distribution of (a) torsional bond 9, (b) torsional bond 10, under stress and constant pressure at 300 K

the $\pm 180°$ region was found to be very high, when considering that the energy in this region is almost 3 kcal mol^{-1} higher than the minima. *Figure 8b* shows how Φ_4 is affected by the application of a tensile force. The $-70°$ region predominates, while on compression the 50° region of the torsional angles predominates. The $\pm 180°$ region remains constant under compressive and tensile stress. The torsional angle Φ_4 at 300 K populates the 60° region, which has a high energy value of 2–3 kcal mol^{-1}. The same conclusions can be drawn when evaluating plot $\Phi_4\Phi_5$ (which is not shown). This plot also has one minima region, which is below 1 kcal mol^{-1}, situated at $-70°$.

The energy contour maps, $\Phi_4\Phi_5$ (not shown), $\Phi_5\Phi_6$ (*Figure 4*), and $\Phi_5\Phi_9$ (not shown), show minima at torsional values of 120 and -100, ± 120 and 70, and $-50°$, respectively. A wide range of Φ_5 values from the crystal search is seen. Φ_5 shows complex torsional distribution due to the three neighbouring torsional angles in relation to it. At 300 K, the results for Φ_4 (*Figure 8b*) show a greater population in the regions -60, 70, and $-170°$. These Φ_4 values correspond to high energy regions (2–3 kcal mol^{-1}) for Φ_5 at 120, -130 and 80, and -110 and 70° (50–120°) on the energy plot $\Phi_4\Phi_5$ (not shown). If, however, these values are compared with the energy plot $\Phi_5\Phi_6$, they coincide with all of the minima regions (see *Figure 4*). Therefore, the overall population of Φ_5 (see *Figure 9a*) is dictated by the numerous minima regions in the $\Phi_5\Phi_6$ plot and the two minima regions in the $\Phi_4\Phi_5$ plot. The energy values for Φ_4 at $-70°$ is between 0–1 kcal mol^{-1}, which corresponds to $-100°$ and (100–140°) for Φ_5. When Φ_5 is subjected to a compressive stress, major peaks reside at -130, -100, 70, and $-70°$ (see *Figure 9a*). This relates to the compression values of Φ_4, Φ_6 and Φ_9. On expansion, the highest peak is at $-80°$ for Φ_5 (see *Figure 9a*); the positive region shows a broad population from 50 to 140°. The single torsional value of $-80°$ for Φ_5 only corresponds with a region on the $\Phi_5\Phi_9$ plot at 2–3 kcal mol^{-1}. The broad regions relate to the expansion values of Φ_4, Φ_6 and Φ_9.

The energy contour plot for $\Phi_5\Phi_6$ (*Figure 4*) contains four minima regions at ± 120 and $\pm 60°$, while $\Phi_6\Phi_9$ (not shown) has two deep minima wells at -50 and $-70°$. These regions are supported by the crystal data. *Figure 4* shows two pairs of degenerate states, namely those at 120 and $-60°$, and those at -120 and 60°. *Figure 9b* shows the overall population distribution of Φ_6 to be a tetra-modal system. The population distribution of Φ_6 is dependant on Φ_5 and Φ_9, and since the contour plot for $\Phi_6\Phi_9$ is not shown, the population migration will be explained with reference to *Figure 4*. As mentioned above, the positive region for Φ_5 predominates on expansion. From *Figure 4*, this corresponds to an increase in population of -60 and 120°, as can be seen in *Figure 9b*. On the application of a compressive stress, the negative region dominates, which should correspond to an increase in the 60 and $-120°$ population of Φ_6. This is also clearly seen in *Figure 9b*.

The $\Phi_7\Phi_8$ energy plot is a degenerate tetra-modal system. The energy contour map shows the minima to be at ± 60 and $\pm 120°$. The energy barriers between these minima regions is $\leqslant 5$ kcal mol^{-1}. Owing to the steepness of the energy minima well, the population of a region is very much dependent on the starting conformation and temperature. Taking the distribution of $\Phi_7\Phi_8$ as a whole in *Figure 10a*, all of the regions are occupied. The regions occupied by the $\Phi_7\Phi_8$ do not change under the application of stress, but there appears to be a broader distribution in the population under tensile stress. The crystal data[17] values for Φ_7 and Φ_8 are 64.301 and 49.01°, which are in good agreement with our values. Other studies[11,18], using molecular mechanics, also show excellent agreement with these values.

The low energy regions on the $\Phi_9\Phi_{10}$ energy contour map are very broad. These regions range from 60 to 140° and from -120 to $-50°$ for energies <1 kcal mol^{-1} for Φ_9. The torsional angle Φ_9 as for Φ_5, has three neighbouring torsional angles which affect the torsional angle population distribution. Φ_9 is coupled to Φ_5, Φ_6 and Φ_{10}, and analysis of $\Phi_5\Phi_9$ (not shown) and $\Phi_9\Phi_{10}$, confirms the states in which Φ_9 resides under the various conditions. As will be mentioned in the discussion of Φ_{10}, the population for the 300 K distribution resides at $\pm 180°$. In *Figure 6*, the minima for Φ_9 reside between $\pm$(60–130°), but the $\Phi_5\Phi_9$ plot (not shown) shows a high energy of ~ 3 kcal mol^{-1}, for the same Φ_9 values. The highest population peak for Φ_9 under compression is at 90°. If Φ_{10} resides at $-70°$ under these conditions, it can be seen in *Figure 6* that Φ_9 resides in a very broad energy region (<1 kcal mol^{-1}) at $\sim \pm 100°$. There is also a corresponding mode at the same energy for plot $\Phi_5\Phi_9$. On expansion, the torsional Φ_9 population coalesces to a bi-modal system, thus forming a broad distribution of torsions in the regions which are depicted in *Figure 11a*. The torsional angle population of Φ_9 is evenly distributed. These conformations for Φ_9 correspond to high energy modes of 2–3 kcal mol^{-1} in $\Phi_5\Phi_9$ and $\Phi_9\Phi_{10}$.

Table 2 Averaged geometric values of bond lengths (Å) and bond angles (°) for structural motifs under various conditions

Bond/angle	300 K	Compression stress	Tensile stress
N1–N2 N3–N4	3.43±0.36	3.34±0.32	3.38±0.35
N2–Cα N3–Cα	8.07±1.01	7.75±0.89	9.03±0.56
N2–N3	12.66±2.52	11.03±0.82	15.57±1.0
N2–Cα–N3	60	60	130
N1–N2–Cα	90	150	120
N4–N3–Cα	70/110	110	120

The contour map for $\Phi_9\Phi_{10}$ shows minima at torsional values of $\pm 180°$. Φ_{10} is a tri-modal system, with a very broad region (< 1 kcal mol^{-1}) around the minima. There are also two further minima regions at $\pm 70°$, which are not degenerate because of the lack of symmetry of the energy contour about that region (see *Figure 6*). There is a greater area occupied at $-70°$ for energies which are less than 1 kcal mol^{-1}. The total number of modes, for the molecular dynamics experiment, is also three, and the population coincides with the energy contour map. As a tensile stress is applied, the population at a torsional value of $\pm 180°$ decreased, while the region at 70° increased. When a compressive stress is applied to the system, the $-70°$ region increases at the expense of the $\pm 180°$ region.

Virtual bonding

The lengths (N1–N2, N2–Cα, N3–Cα), and angles (N1–N2–Cα, N2–Cα–N3, Cα–N3–N4), shown in *Figure 1*, are dependent on all of the torsional angles, with Φ_6 being the exception. The latter adopts a conformation with respect to the neighbouring torsions Φ_5 and Φ_9. *Table 2* summarizes the bond lengths and angles of interest in the link molecule.

Table 2 shows the average and standard deviation of virtual bond lengths (in Å). The virtual bond lengths have been averaged for the various conditions. (N1–N2/N3–N4 and N2–Cα/N3–Cα are considered to represent the same structural motif, and therefore these pairs are averaged together.) Where more than one value is given for the bond angles, this indicates a multipeak distribution. The values are in decreasing order of population.

On the application of a stress, the N1–N2/N3–N4 structural motifs show very little deviation away from the mean values, which are themselves relatively constant, at 3.38 Å. This is consistent with the fact that the Φ_9 and Φ_{10} populations show equal and opposite torsional values under both stress conditions. The result is no net change in the virtual bond lengths under both stress conditions.

However, the N2–Cα and N3–Cα distances result in a noticeable increase in virtual bond length when a tensile stress is applied, which suggests a net torsional angle population shift from 90° to 180° for Φ_1–Φ_8. This means that the minima for these torsional angles reside at torsional angle values which are closer to 90° (or less) than to 180°. This is true for the torsional values Φ_1 to Φ_6 (except for Φ_4). The N2–Cα and N3–Cα average of 8.3 Å is ~1 Å less than the value obtained by Lovell and Windle[1] . This is due to the higher energy levels that are occupied at 300 K. On the application of a stress, these segments show characteristic motions in response to the relevant stress.

The large deviation for N2–N3 of 2.5 Å is an indication of how flexible the torsional angles Φ_1–Φ_6 are. In these cases, only very subtle shifts in torsional angle values can result in large deviations from the mean value.

On the application of a compressive stress, the responses of N1–N2–Cα and N3–N4–Cα are slightly different at 300 K; N3–N4–Cα shows a bi-modal response at the values given in *Table 2*, while N1–N2–Cα shows an intermediate value. When a compressive and tensile stress is applied, the response appears to be the same in both cases, with a shift to ~120°. These virtual bond angles appear to be insensitive to changes in stress, which may be due to the zero net stress response of N1–N2 and N3–N4.

The response of N2–Cα–N3 corresponds to the stresses applied to the link molecule. On expansion, this torsional bond angle increases, while on compression, a decrease in the angle is observed. The virtual bond angle values for N2–Cα–N3 at ~50° are very small when compared to the value obtained by Lovell and Windle (110°)[13]. This is due to our different minima sites for the torsional angles Φ_1 to Φ_6.

CONCLUSIONS

This study demonstrates how each torsional angle in a linear epoxy system varies with the application of stress. They all demonstrate a population migration from a lower energy to a higher energy state on the application of an external stress, with the exception of Φ_7 and Φ_8. The Φ_6 torsional angle is the only one which is not directly forming the main chain of the link molecule, and it can be concluded that its motion is due to the motions of Φ_5 and Φ_9. Subtle changes in the torsional angle values can result in large changes in the virtual bond lengths N2–Cα and N3–Cα, while N1–N2 and N3–N4 appear to be largely unaffected under similar conditions. This is due to the minima that each torsional angle possesses. The response of angles N1–N2–Cα and N4–N3–Cα is due to the orientation of the torsional angles between N2–Cα and N3–Cα. The angle N2–Cα–N3 shows a clear and positive response to the type of external stress applied, i.e. increasing and decreasing on the application of tensile and compressive stresses, respectively.

ACKNOWLEDGEMENTS

We would like to thank the materials and Structures Department, Defence Research Agency, Farnborough for financial support, and Dr Lovell for helpful discussions. We should also like to thank Terry Knowles for his help in the CDB fragment search and Richard Heald for writing some of the analysis software.

REFERENCES

1 Mark, H. F., Gaylord, N. G. and Bikales, N. M. (Eds) 'Encyclopedia of Polymer Science and Technology—Plastics, Resins, Rubbers and Fibres', Vol. 6, Wiley, New York, p. 209, and references therein

2 Dyson, R. W. (Ed.) 'Engineering Polymers', Blackie, Glasgow, 1990, and references therein

3 Buist, G. J., Hagger, A. J., Howlin, B. J., Jones, J. R., Parker, M. J., Barton, J. M. and Wright, W. W. *Polym. Commun.* 1990, **31**. 265

4 Buist, G. J., Hagger, A. J., Jones, J. R., Barton, J. M. and Wright, W. W. *Polym. Commun.* 1988, **29**, 5

5 Fischer, A., Schlothauer, K., Pfitzmann, A. and Spevacek, J. *Polymer* 1992, **33**, 1370

6 Buist, G. J., Hagger, A. J., Howlin, B. J., Jones, J. R., Parker, M. J., Barton, J. M. and Wright, W. W. *Polym. Commun.* 1990, **31**, 265

7 Liu, S., Buist, G. J., Hammerton, I., Howlin, B. J., Jones, J. R. and Barton, J. M. *J. Mater. Chem.* 1994, **4**, 379

8 Liu, S., Buist, G. J., Hammerton, I., Howlin, B. J., Jones, J. R. and Barton, J. M. *Polymer* submitted

9 Heyes, D. M., Buist, G. J., Hamerton, I., Howlin, B. J., Jones, J. R. and Barton, J. M. *J. Mater. Chem.* submitted

10 Allen, F. K., Bellard, S. A., Brice, M. D., Cartwright, B. A., Doubleday, A., Higgs, H., Hummelink, T., Hummelink-Peters, B. G., Kennard, O., Motherwell, W. D. S., Rodges, J. R. and Watson, D. G. *Acta Crystallogr. Sect. B* 1979, **35**, 2331

11 Mayo, S. L., Olafson, B. B. and Goddard III, W. A. *J. Phys. Chem.* 1990, **94**, 8897

12 Lovell, R. and Windle, A. H. in 'Computer Simulation of Polymers' (Ed. R. J. Roe), Prentice-Hall, Englewood Cliffs, NJ, 1990, p. 41

13 Lovell, R. and Windle, A. H. *Polymer* 1991, **32**, 2272

14 Gastiger, J. *Tetrahedron* 1980, **36**, 3219

15 Swope, W. C. *J. Chem. Phys.* 1982, **76**, 637

16 Hehre, W. J., Radom, L., Schleyer, P. V. R. and Pople, J. A. 'Ab Initio Molecular Orbital Theory', Wiley, New York, 1986, p. 365

17 Flippen-Andersen, J. L. and Gilardi, R. *Acta Crystallogr. Sect. B* 1981, **37**, 1433

18 Fan, C. F. and Hsu, S. L. *Macromolecules* 1991, **24**, 6244